University of Groningen

Gas desulfurization with ferric chelates of EDTA and HEDTA: New model for the oxidative absorption of hydrogen sulfide

Demmink, J.F; Beenackers, A.A C M

IMPORTANT NOTE: You are advised to consult the publisher's version (publisher's PDF) if you wish to cite from it. Please check the document version below.

Document Version
Publisher's PDF, also known as Version of record

Link to publication in University of Groningen/UMCG research database

Citation for published version (APA):
Demmink, J. F., & Beenackers, A. A. C. M. (1998). Gas desulfurization with ferric chelates of EDTA and HEDTA: New model for the oxidative absorption of hydrogen sulfide: New model for the oxidative absorption of hydrogen sulfide. *Industrial & Engineering Chemistry Research*, *37*(4), 1444-1453. https://doi.org/10.1021/ie970427n

Gas Desulfurization with Ferric Chelates of EDTA and HEDTA: New Model for the Oxidative Absorption of Hydrogen Sulfide

J. F. Demmink and A. A. C. M. Beenackers*

*Department of Chemical Engineering, University of Groningen, Nijenborgh 4,
9747 AG Groningen, The Netherlands*

The experimental data of Wubs and Beenackers (*AIChE J.* **1994**, *40* (3), 433−444) on the oxidative absorption of H_2S into aqueous solutions of ferric chelates of ethylenediaminetetraacetic acid (EDTA) and hydroxyethylethylenediaminetriacetic acid (HEDTA) were reinterpreted using a new penetration model for mass transfer parallel to chemical reaction. Different from the discussion by Wubs and Beenackers (1994), which was based on general, approximate models for the reactive absorption of gases into liquids, it now appears that the diffusivity of ferric chelates of EDTA and HEDTA are in good agreement with the values determined from the reactive absorption of molecular oxygen into aqueous solutions of ferrous EDTA and HEDTA (Wubs and Beenackers, *Ind. Eng. Chem. Res.***1993**, *32*, 2580−2594). Also, it now appears that the data from Wubs and Beenackers (1994) are compatible with ferric chelate complex equilibrium constants, reported elsewhere (for instance, Martell and Smith, *Critical Stability Constants*, 1982). Reinterpretation of the absorption data from Wubs and Beenackers (1994) resulted in the following kinetic rate constants ($T = 293$ K, $C_{Fe(III)} = 78$ mol/m^3 and $2 \leq$ pH $\leq$ 9): EDTA, monohydroxylated complex, $250 \leq k_{1,1} \leq 300$ m^3/(mol s); HEDTA, monohydroxylated complex, $1.4 \leq k_{1,1} \leq 1.6$ m^3/(mol s); HEDTA, dihydroxylated complex, $550 \leq k_{1,1} \leq 650$ m^3/(mol s); for the reaction rate expressed by $-R_{H_2S} = k_{1,1}C_{H_2S}C_{Fe(III)}$.

1. Introduction

Wubs and Beenackers (1994) studied the absorption of H_2S into aqueous solutions of ferric chelates in a stirred cell reactor. The absorption is accompanied by the oxidation of H_2S:

$$H_2S(g) \rightleftarrows H_2S(aq)$$

$$H_2S + 2Fe^{3+}L^{n-} \rightarrow 2Fe^{2+}L^{n-} + 2H^+ + S\downarrow \quad (1)$$
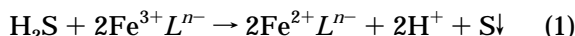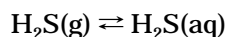
with L^{n-} denoting an organic ligand, in this case ethylenediaminetetraacetic acid (EDTA, $n = 4$) and hydroxyethylethylenediaminetriacetic acid (HEDTA, $n = 3$). The above reaction has found application in gas desulfurization processes (Oostwouder and Hodge, 1995; Nagl, 1997; DeBerry, 1997), where regeneration of a ferrous chelate takes place by oxidation with molecular oxygen, O_2, in a separate vessel. Prominent gas desulfurization processes based on reaction 1 are the SulFerox process, with 40 operating plants in 1995 (Oostwouder and Hodge, 1995), and the LO-CAT/LO-CAT II process. The latter process reported in 1997 to having 140 operating plants, with a total capacity of 3.8 × 10^5 kg of sulfur/day (Cantrall, 1997). Iron chelate based gas desulfurization processes are economically advantageous over other options for sulfur productions between 200 and 20 000 kg/day (Oostwouder and Hodge, 1995).

Although Wubs and Beenackers (1994) revealed the most important aspects that affect the oxidative absorption of H_2S, including the reaction mechanism, and the effect of the structure of ferric chelates (as a function of pH, temperature, T, and ferric chelate concentration,

$C_{Fe(III)}$) on their reactivity, some questions remained. Despite the similar structure of ferric EDTA and HEDTA, and different from observations on the reactive absorption of O_2 (Wubs and Beenackers, 1993) and nitric oxide, NO (Demmink et al., 1997), into aqueous solutions of ferrous EDTA and HEDTA, Wubs and Beenackers (1994) reported a considerable difference in their diffusivity ($D_{Fe(III)L}$): at $T = 295$ K, $D_{Fe(III)L} = 0.16 \times 10^{-9}$ m^2/s for ferric EDTA and $D_{Fe(III)L} = 0.42 \times 10^{-9}$ m^2/s for ferric HEDTA (compare $D_{Fe(II)L} = 0.26 \times 10^{-9}$ m^2/s for both ferrous EDTA and HEDTA, $T = 294$ K, determined from ferrous chelate oxidation by Wubs and Beenackers (1993), as recalculated by Demmink and Beenackers (1997), and $D_{Fe(II)L} = 0.24 \times 10^{-9}$ m^2/s for both ferrous EDTA and HEDTA, $T = 294$ K, determined by Demmink et al. (1997) from reactive absorption of NO). Given the very similar $D_{Fe(II)L}$ for ferrous EDTA and HEDTA (Wubs and Beenackers, 1993; Demmink et al., 1997), it follows that, for these large complexes, $D_{Fe(II)L}$ depends on molecular mass, rather than charge of the complex. Therefore, the $D_{Fe(III)L}$ values for ferric EDTA and HEDTA should be identical as well, and the $D_{Fe(III)L}$ values determined by Wubs and Beenackers (1994) need to be reconsidered.

As a result of a maximum in the reactivity of ferric EDTA, as a function of pH, that was not understood from ferric EDTA complex chemistry, Wubs and Beenackers (1994) reported a large uncertainty in the reactivity of ferric EDTA; see Table 1. Furthermore, as shown in Table 2, the equilibrium constant (K_e, with e pertaining to the equation in this work, defining the equilibrium, see Table 2) for one of the ferric EDTA species, as determined from the gas absorption data, differed significantly from its literature value (Martell

* To whom correspondence may be addressed.

Table 1. Reaction Rate Constants $k_{1,1}$ Determined from Data of Wubs and Beenackers (1994), $T = 294$ K, $C_{Fe(II)} = 0.078$ kmol/m³

reactant		$k_{1,1}{}^a$ (m³/(mol s))	$k_{1,1}{}^b$ (m³/(mol s))
$Fe^{3+}L_{EDTA}^{4-}$	(m0)	≈0	≈0
$Fe^{3+}L_{EDTA}^{4-}$ (OH⁻)	(m1)	250–300	14–21
$Fe^{3+}L_{HEDTA}^{3-}$	(m0)	≈0	≈0
$Fe^{3+}L_{HEDTA}^{3-}$ (OH⁻)	(m1)	1.5	1.8
$Fe^{3+}L_{EDTA}^{3-}$ (OH⁻)₂	(m2)	550–650	130

[a] This work. [b] Reported by Wubs and Beenackers (1994).

Table 2. Equilibrium and Forward Rate Constants, Ferric EDTA and HEDTA, for Equilibrium e, $T = 298$ K ($pK_e = -\log K_e$)

e	i^a	$pK_e{}^{b,c}$ EDTA	$pK_e{}^{b,c}$ HEDTA	$k_e{}^{d,e}$ EDTA	$k_e{}^{d,e}$ HEDTA
20		7.58,[b1] 6.22[b3]	4.11,[b1] 4.4[b3]	fast	fast
21			8.69,[b1] 8.68[b3]	fast	fast
22		−2.95[b1]	−2.38,[b1] −2.3[b3]	0.6	0.9
23		4.63[b4]	1.73[b4]	20	60
25	4	1.95[b2]		fast	fast
25	3	2.68[b2]	2.60[b2]	fast	fast
25	2	6.11[b2]	5.39[b2]	fast	fast
25	1	10.17[b2]	9.81[b2]	fast	fast

[a] Pertaining to protonation, see eq 25. [b1] Gustafson and Martell (1963). [b2] Martell and Smith (1982). [b3] Wubs and Beenackers (1994), from gas absorption data. [b4] $K_{23} = K_{20}K_{22}$. [c] kmol/m³ (eqs 20, 21, and 25); m³/kmol (eq 22); () (eq 23). [d] Wilkins and Yelin (1969). [e] Forward reaction rate constants; m³/(mol s) (eqs 22 and 23); 1/s (eqs 20, 21, and 25).

and Smith, 1982), whereas the equilibrium constants for ferric HEDTA matched the literature values very well.

Recently, we showed how near interface concentration and pH gradients caused by mass-transfer resistances may affect the reactive absorption of O_2 and NO into solutions of ferrous nitrilotriacetic acid (NTA) (Demmink and Beenackers, 1997; Demmink et al., 1997, respectively). A key role in the reactive absorption of a gas into ferrous NTA solutions appeared to be played by the many different iron chelate species present at the gas−liquid interface, each showing a specific reactivity to the absorbing gas. Near interface interconversion of iron chelates, resulting from the consumption of the most reactive species, was shown to be of importance. Here, we present a new comprehensive model for the reactive absorption of H_2S into ferric chelate solutions, based on mass transfer parallel to a set of complex chemical reactions. It will be shown that near interface concentration gradients substantially affect the gas absorption rate. As a result of this approach, the experimental data of Wubs and Beenackers (1994) become much more consistent with literature data on equilibrium constants and diffusion coefficients than it seemed previously.

2. Model Development

The rate of absorption of H_2S per unit of gas−liquid interface, J_A, is given by (Westerterp et al., 1984)

$$J_A = k_L E_A (C_{AL}^i - \bar{C}_A) \quad (2)$$

with k_L the liquid-side mass-transfer coefficient, $C_{A,L}^i$ the liquid-side interfacial H_2S concentration and $\bar{C}_A$ the concentration of H_2S in the liquid bulk (i.e., at $x \to \infty$ with x the distance from the gas−liquid interface). The

enhancement factor E_A is the result of chemical reaction and is defined by the above eq 2. It can be shown that, for the data considered in this work, $\bar{C}_A = 0$.

At any time between 0 and an average contact time θ, defined by (Westerterp et al., 1984)

$$\theta = \frac{4D_A}{\pi k_L{}^2} \quad (3)$$

J_A is given by (Westerterp et al., 1984):

$$J_A(t) = -D_A \left(\frac{\partial C_A}{\partial X} \right)_{x=0,t} \quad (4)$$

The average (i.e., observed) absorption rate now follows from

$$\bar{J}_A = \frac{1}{\theta} \int_0^\theta J_A(t)\, dt \quad (5)$$

and the observed E_A from (Westerterp et al., 1984):

$$E_A \equiv \frac{\bar{J}_A}{k_L C_{A,L}^i} = \frac{D_A}{k_L C_{A,L}^i \theta} \int_0^\theta \left[\left(\frac{\partial C_A}{\partial X} \right)_{x=0,t} \right] dt \quad (6)$$

Calculation of the time-dependent concentration gradient $(\partial C_A/\partial x)_{x=0,t}$ asks for mass balances over the mass-transfer zone for H_2S as well as for all ionic species present (Newman, 1973). In combination with the dynamic charge balance, these mass balances may be rewritten in dimensionless form to (Demmink and Beenackers, 1997):

$$\frac{\partial \xi_i}{\partial \tau} = \frac{\partial}{\partial r_p} \left(\frac{2\tau\Gamma_i}{\pi} \frac{\partial \xi_i}{\partial r_p} - \frac{2\tau}{\pi}\Gamma_i z_i \xi_i \frac{\sum z_j \Gamma_j \frac{\partial \xi_j}{\partial r_p}}{\sum z_m{}^2 \Gamma_m \xi_m} \right) + \frac{2\tau\theta R_i}{C_{A,L}^i} \quad (7)$$

with z_i the charge of ionic species i, $C_{A,L}^i$ the liquid-side interfacial H_2S concentration, and

$$\xi_i = \frac{C_i}{C_{A,L}^i} \quad (8)$$

$$\Gamma_i = \frac{D_i}{D_A} \quad (9)$$

$$r_p = \frac{X}{\sqrt{\pi D_A \theta}} \quad (10)$$

$$\tau = \sqrt{\frac{t}{\theta}} \quad (11)$$

In order to maintain electroneutrality throughout the mass-transfer zone, for one of the ionic components, eq 7 is replaced by the electroneutrality equation

$$\sum_{i=1}^{N} z_i \xi_i = 0 \quad (12)$$

Finally, the water equilibrium is assumed to be satisfied

throughout the mass-transfer zone (Caldin and Gold, 1975):

$$C_{H^+} = \frac{K_W}{C_{OH^-}} \quad (13)$$

with K_W values given by CRC (1980). Boundary conditions for all nonvolatile species are given by

$$\left. \begin{array}{l} \tau \geq 0 \\ r_p = 0 \end{array} \right\} \quad \left(\frac{\partial \xi_i}{\partial r_p} \right) = 0 \quad (14)$$

$$\left. \begin{array}{l} \tau \geq 0 \\ r_p \to \infty \end{array} \right\} \quad \xi_i = \bar{\bar{\xi}}_i \quad (15)$$

$$\left. \begin{array}{l} \tau = 0 \\ r_p \geq 0 \end{array} \right\} \quad \xi_i = \bar{\bar{\xi}}_i \quad (16)$$

and for H_2S:

$$\left. \begin{array}{l} \tau \geq 0 \\ r_p = 0 \end{array} \right\} \quad \xi_A = 1 \quad (17)$$

$$\left. \begin{array}{l} \tau \geq 0 \\ r_p \to \infty \end{array} \right\} \quad \xi_A = 0 \quad (18)$$
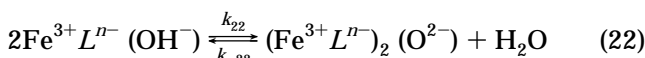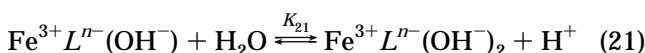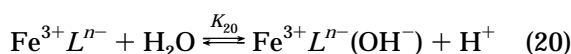
$$\left. \begin{array}{l} \tau = 0 \\ r_p > 0 \end{array} \right\} \quad \xi_A = 0 \quad (19)$$

with $\bar{\bar{\xi}}_i$ the dimensionless concentration of species i in the liquid bulk. Numerical solution of the set of eqs 7 with boundary conditions (14)−(16) and (17)−(19), in combination with electroneutrality condition (12), gives the concentrations of all components in a liquid element, as a function of τ and r_p. For this purpose, NAG Routine D03PGE (NAG Fortran Library) was used on a Cray J932.

The approach described above enables the calculation of E_A, accounting for (1) local concentration gradients of all ionic species; (2) near interface interconversion of ferric chelates resulting from chemical equilibria and consumption of the more reactive ferric species by H_2S; (3) ionic diffusion, including the static and dynamic electroneutrality conditions; (4) the reaction kinetics for (1).

Information on the reaction mechanism, including the role of ferric chelate complex chemistry, now is required.

2.1. Complex Chemistry of Ferric Chelates. Philip and Brooks (1974) observed for ferric HEDTA complex that reaction 1 is strongly pH dependent. They attributed this pH dependence to the formation of hydroxylated and μ-oxo-bridged ferric chelates at high pH. These ferric complexes were observed by Gustafson and Martell (1963), Schugar et al. (1969), and Wilkins and Yelin (1969):

$$Fe^{3+}L^{n-} + H_2O \underset{}{\overset{K_{20}}{\rightleftharpoons}} Fe^{3+}L^{n-}(OH^-) + H^+ \quad (20)$$

$$Fe^{3+}L^{n-}(OH^-) + H_2O \underset{}{\overset{K_{21}}{\rightleftharpoons}} Fe^{3+}L^{n-}(OH^-)_2 + H^+ \quad (21)$$

$$2Fe^{3+}L^{n-}(OH^-) \underset{k_{-22}}{\overset{k_{22}}{\rightleftharpoons}} (Fe^{3+}L^{n-})_2(O^{2-}) + H_2O \quad (22)$$

with K_{20}, K_{21}, and K_{22} (=k_{22}/k_{-22}, with k_{22} and k_{-22} the forward and backward reaction rate constants, respec-
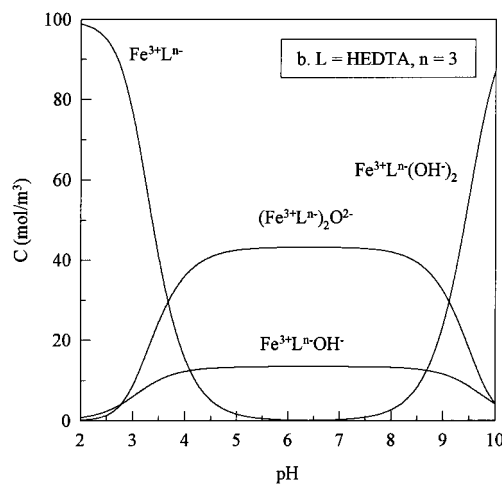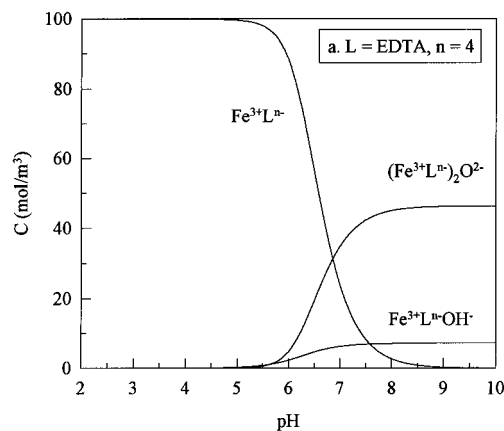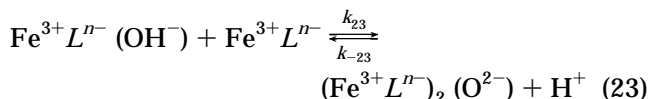

Figure 1. Concentration of ferric chelates, $T = 293$ K, $C_{Fe(III)} = C_{ligand} = 0.100$ kmol/m^3, equilibrium constants from Gustafson and Martell (1963), given in Table 2. (a) ferric EDTA; (b) ferric HEDTA.

tively) given in Table 2. Equilibrium 22 may also be established through

$$Fe^{3+}L^{n-}(OH^-) + Fe^{3+}L^{n-} \underset{k_{-23}}{\overset{k_{23}}{\rightleftharpoons}}$$
$$(Fe^{3+}L^{n-})_2(O^{2-}) + H^+ \quad (23)$$

where $k_{-22} < k_{-23}$ (Wilkins and Yelin, 1969; see Table 2). Dissociation of the μ-oxo dimer therefore is acid-catalyzed. It should be noted that

$$K_{23} = \frac{k_{23}}{k_{-23}} = K_{22}K_{20} \Rightarrow k_{-23} = \frac{k_{23}}{K_{22}K_{20}} \quad (24)$$

with K_{22}, k_{23}, and K_{20} reported in literature; see Table 2. Figure 1 shows the concentrations of the ferric ions as a function of pH, for ferric EDTA and HEDTA.

Philip and Brooks (1974) concluded that hydroxylated species formed in eqs 20 and 21 are far more reactive to H_2S than nonhydroxylated species. It was suggested that μ-oxo-bridged ferric chelates $(Fe^{3+}L^{n-})_2O^{2-}$ are not reactive; they may participate in reaction 1 through dissociation, eqs 22 and 23 only. The phenomenon of increasing reactivity of ferric chelates with hydroxylation was shown by Asai et al. (1990, 1997) ($L = H_2O$), DeBerry et al. (1991), Wubs and Beenackers (1994), and Neyaglov et al. (1991) ($L =$ EDTA and HEDTA), Demmink et al. (1994) ($L =$ NTA), and Yao and Millero (1996) (ferric oxide precipitates).

Table 3. Characteristics of Studies of the Reaction between H₂S and Ferric Chelates

| author	system[a]	ligand	T (K)	pH	$C_{Fe(III)}$ (kmol/m³)	$C_L/C_{Fe(III)}$	$C_{H_2S}{}^b$ (kmol/m³)	order Fe(III)	order H₂S
Philip and Brooks (1974)	A1, s2	HEDTA	298	6.5−7		1.02	10^{-4}−10^{-2}	c	
Neumann and Lynn (1984)	B2, s6	NTA	333−338	3.5−4.0	0.4	1.1			
	B3, s5	NTA	333−338	3.9−4.1	0.10	1.1	$<4 \times 10^{-3}$ [d]		
Koch et al. (1986)	A1, s2	EDTA DTPA		9.5					
Asai et al. (1990)	B1, s5	H₂O	298−313	1−3	0.01−0.07		0.2−2[d]	1	1
DeBerry et al. (1991)	A1, s2,3	EDTA DTPA HEDTA EGTA	283	6−8	$(2.5−25) \times 10^{-4}$	1	$(2.5−10) \times 10^{-4}$	1	1
Neyaglov et al. (1991)	A1, s2	EDTA	293−323	7−9.5	$(0.2−0.8) \times 10^{-3}$	1	0.48×10^{-3}	1	1
dos Santos Afonso and Stumm (1992)[e]	B2, s5	H₂O	298	4−7	$(1.27−2.69 \times 10^{-4}$ [f]		0.1−1[d]		
DeBerry (1993)	A1, s2,3	EDTA DTPA HEDTA EGTA CDTA NTA	283	6−8	$(0.25−25) \times 10^{-3}$	1	0.25−10	1	1
Wubs and Beenackers (1994)	B1, s1	EDTA HEDTA	293−333	3−9	0.040−0.150	1.1	(1×10^{-3})−(0.070)	1	1
Demmink et al. (1994)	B4, s4	NTA	286	6−8	0−0.200	2	0−0.43	1	1
Giles et al. (1994)	A1, s2	EDTA	273−323	6−10				0−2	
Wubs (1994)	B1, s1	NTA	295	7	0.03	2	$(1−50) \times 10^{-3}$	0−1	1
Clarke et al. (1994)	B2, s8	NTA		7−8.5	0.02	2			
Lonergan et al. (1995)	A1, s2,3	EDTA		10.5					
Yao and Millero (1996)[e]	A2, s7	H₂O	277−320	4−8.5	$(4−6) \times 10^{-5}$ [g]		0.025	1	1

[a] Single-phase systems: A1, stopped flow; A2, stirred vessel. Two-phase systems: B1, stirred cell reactor; B2, bubble column; B3, wetted-wall column; B4, co-current downflow column packed with static mixers. H₂S detection: sl, pressure indicator; s2, spectrofotometer; s3, sulfide ion electrode; s4, lead acetate based H₂S detector; s5, Fe³⁺ conversion; s6, soap-bubble flowmeter; s7, titration; s8, laser desorption mass spectroscopy. [b] $C_{A,L}^i$ in multiphase studies. [c] Not reported. [d] Not reported in original paper, estimated from solubility in water. [e] Fe(OH)₃ precipitates. [f] Pertaining to surface. [g] Pertaining to total iron content.

If a ligand is present in excess, the following set of equilibria occur:

$$H_i L^{(n-i)-} \underset{}{\overset{K_{25,i}}{\rightleftharpoons}} H_{i-1} L^{(n-i+1)-} + H^+ \qquad (25)$$
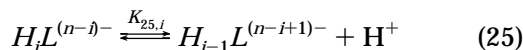
with $i = 1 \dots n$; see Table 2.

2.2. Reaction Mechanism. Although iron chelates are widely used for gas desulfurization, actual kinetic data and mechanistic studies are limited. Table 3 gives an overview. Mechanistic studies by Koch et al. (1986), Neyaglov et al. (1991), and Lonergan et al. (1995) revealed the existence of a meta-stable ferric sulfide complex, whose formation may be given by

$$Fe^{3+}L^{n-} + H_2S \underset{k_{-26}}{\overset{k_{26}}{\rightleftharpoons}} Fe^{3+}L^{n-} (SH^-) + H^+ \quad (26)$$
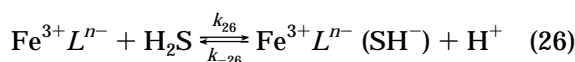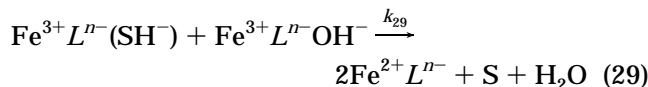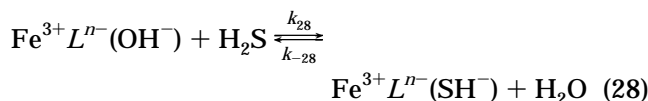
Similar ferric sulfide intermediates were suggested by dos Santos Afonso and Stumm (1992) and Yao and Millero (1996) for Fe(OH)₃ precipitates (surface reaction).
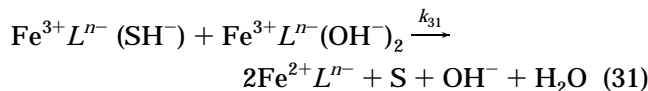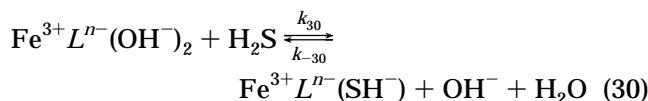
Despite disagreement on the details of the consecutive step, which may involve either a sulfhydryl radical HS• (Neyaglov et al., 1991; Lonergan et al., 1995) or an internal electron transfer (Koch et al., 1986; Wubs and Beenackers, 1994), all schemes proposed assume that $Fe^{3+}L^{n-}$ (SH⁻) effectively reacts according to

$$Fe^{3+}L^{n-}(SH^-) + Fe^{3+}L^{n-} \overset{k_{27}}{\longrightarrow}$$
$$2Fe^{2+}L^{n-} + S + H^+ \quad (27)$$
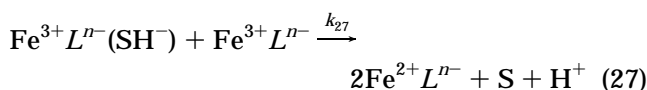
The high reactivity observed at elevated pH indicates that reactions 26 and 27 may also involve hydroxylated species:

$$Fe^{3+}L^{n-}(OH^-) + H_2S \underset{k_{-28}}{\overset{k_{28}}{\rightleftharpoons}}$$
$$Fe^{3+}L^{n-}(SH^-) + H_2O \quad (28)$$

$$Fe^{3+}L^{n-}(SH^-) + Fe^{3+}L^{n-}OH^- \overset{k_{29}}{\longrightarrow}$$
$$2Fe^{2+}L^{n-} + S + H_2O \quad (29)$$

and for ferric HEDTA

$$Fe^{3+}L^{n-}(OH^-)_2 + H_2S \underset{k_{-30}}{\overset{k_{30}}{\rightleftharpoons}}$$
$$Fe^{3+}L^{n-}(SH^-) + OH^- + H_2O \quad (30)$$

$$Fe^{3+}L^{n-} (SH^-) + Fe^{3+}L^{n-}(OH^-)_2 \overset{k_{31}}{\longrightarrow}$$
$$2Fe^{2+}L^{n-} + S + OH^- + H_2O \quad (31)$$

All literature studies (see Table 3) report reaction 1 to proceed first-order in Fe(III) and H₂S. As shown below, all ferric chelate consuming steps take place within the reaction zone, and therefore, forward reactions 26, 28, and 30 are rate-determining. This can be shown from simplified rate expressions, assuming steady state in the concentration $Fe^{3+}L^{n-}(SH^-)$, and independent reaction pathways for $Fe^{3+}L^{n-}$, $Fe^{3+}L^{n-}(OH^-)$, and $Fe^{3+}L^{n-}(OH^-)_2$. With m0, m1, and m2 pertaining to the complexes $Fe^{3+}L^{n-}$, $Fe^{3+}L^{n-}(OH^-)$,

and $Fe^{3+}L^{n-}(OH^-)_2$, respectively, it follows for (26) and (27)

$$-R_A^{(m0)} = k_{26} \left(\frac{\left(\frac{k_{27}C_H^{(m0)}}{k_{-26}C_{H^+}} \right)}{\left(\frac{k_{27}C_H^{(m0)}}{k_{-26}C_{H^+}} \right) + 1} \right) C_A C_B^{(m0)} \qquad (32)$$

with asymptotic solutions

$$\frac{k_{27}C_B^{(m0)}}{k_{-26}C_{H^+}} \gg 1 \Rightarrow -R_A^{(m0)} = k_{26}C_A C_B^{(m0)} \equiv$$

$$k_{1,1}^{(m0)} C_A C_B^{(m0)} \quad (33)$$

$$\frac{k_{27}C_B^{(m0)}}{k_{-26}C_{H^+}} \ll 1 \Rightarrow -R_A^{(m0)} = \frac{k_{26}k_{27}}{k_{-26}C_{H^+}} C_A (C_B^{(m0)})^2 \quad (34)$$

while for reactions 28 and 29 it follows that

$$-R_A^{(m1)} = k_{28} \left(\frac{\left(\frac{k_{29}C_B^{(m1)}}{k_{-28}} \right)}{\left(\frac{k_{29}C_B^{(m1)}}{k_{-28}} \right) + 1} \right) C_A C_B^{(m1)} \qquad (35)$$

with asymptotic solutions

$$\frac{k_{29}C_B^{(m1)}}{k_{-28}} \gg 1 \Rightarrow -R_A^{(m1)} = k_{28}C_A C_B^{(m1)} \equiv$$

$$k_{1,1}^{(m1)} C_A C_B^{(m1)} \quad (36)$$

$$\frac{k_{29}C_B^{(m1)}}{k_{-28}} \ll 1 \Rightarrow -R_A^{(m1)} = \frac{k_{28}k_{29}}{k_{-28}} C_A (C_B^{(m1)})^2 \quad (37)$$

and for reactions 30 and 31

$$-R_A^{(m2)} = k_{30} \left(\frac{\left(\frac{k_{31}C_B^{(m2)}}{k_{-30}C_{OH^-}} \right)}{\left(\frac{k_{31}C_B^{(m2)}}{k_{-30}C_{OH^-}} \right) + 1} \right) C_A C_B^{(m2)} \qquad (38)$$

with asymptotic solutions

$$\frac{k_{31}C_B^{(m2)}}{k_{-30}C_{OH^-}} \gg 1 \Rightarrow -R_A^{(m2)} = k_{30}C_A C_B^{(m2)} \equiv$$

$$k_{1,1}^{(m2)} C_A C_B^{(m2)} \quad (39)$$

$$\frac{k_{31}C_B^{(m2)}}{k_{-30}C_{OH^-}} \ll 1 \Rightarrow -R_A^{(m2)} = \frac{k_{30}k_{31}}{k_{-30}C_{OH^-}} C_A (C_B^{(m2)})^2 \quad (40)$$

The above expressions (32), (35), and (38) refer to concentrations of specific ferric chelates ($C_B^{(m0)}$, $C_B^{(m1)}$, and $C_B^{(m2)}$), whose values relative to $C_{Fe(III)}$ are a function of $C_{Fe(III)}$ and pH. At high $C_{Fe(III)}$, μ-oxo dimers exist. If these are not reactive to H_2S, as suggested by Philip and Brooks (1974) and Wubs and Beenackers (1994), the observed order in $C_{Fe(III)}$ may be lower than the actual order in $C_B^{(m0)}$, $C_B^{(m1)}$, and $C_B^{(m2)}$, as ($C_B^d/C_{Fe(III)}$) increases with increasing $C_{Fe(III)}$ (also see Wubs and Beenackers, 1994). Despite the large range in $C_{Fe(III)}$

and pH, reported in Table 3, second order in $C_{Fe(III)}$ was never observed, and asymptotic solutions (33), (36), and (39) appear to be valid.

Also taking place at the gas–liquid interface:

$$H_2S \overset{K_{41}}{\rightleftharpoons} HS^- + H^+ \qquad (41)$$

with K_{41} from Tsonopoulos et al. (1976). Asai et al. (1990) and DeBerry (1993) observed reaction 1 to be practically independent of the ionic strength. From this observation DeBerry (1993) concluded that one of the reactants is uncharged, indicating that the formation of $Fe^{3+}L^{n-}(SH^-)$ proceeds through H_2S, rather than HS^-.

It must be realized that expressions (32), (35), and (38) are useful, yet crude approximations. The proposed approach of using pH-independent $k_{1,1}$ values in eqs 32, 35, and 38 is rather empirical. An important assumption is that the interaction between the reaction pathways (26 and 27, 28 and 29, and 30 and 31) may be neglected. As seen in Figure 1, for ferric EDTA at 5.5 ≤ pH ≤ 8 and for ferric HEDTA at 3 ≤ pH ≤ 4.5, both $C_B^{(m0)} > 0$ and $C_B^{(m1)} > 0$. Therefore, forward reaction 26 may not only be followed by reaction 27 and backward reaction 26, but also by reaction 29 and backward reaction 28. Reaction 28 may now be followed by reactions 27 and 29 and backward reactions 26 and 28. If both $C_B^{(m1)} > 0$ and $C_B^{m2} > 0$, as is the case for ferric HEDTA, pH > 8, (28) may be followed by (29) and (31) and backward reactions 28 and 30; (30) may now be followed by reactions 29 and 31 and backward reactions 28 and 30. Also, the pH-dependent role of polysulfides is not included in eqs 32, 35, and 38.

Polysulfides. Clarke et al. (1994) showed that, as a result of reaction 1, monosulfide may polymerize to polysulfides, S_y^{2-}, with $y = 2-7$. It was shown that ferric chelate is required in sulfur polymerization. However, the precise role of the ferric chelate in sulfur polymerization, or the role of polysulfides in H_2S absorption, was not revealed. We therefore propose the use of observed $k_{1,1}$ values. Since the stability of polysulfides appears to be pH-dependent (Clarke et al., 1994), their effect on $k_{1,1}$ possibly is a function of pH as well.

3. Results and Discussion

3.1. High-Pressure Regime. Figure 2 shows near interface concentration gradients calculated from (7) and (12), induced by the absorption of H_2S at a relatively high $C_{A,L}^i$, $C_{A,L}^i = 10$ mol/m³, while $\bar{C}_{Fe(III)} = 97$ mol/m³, $D_{Fe(III)L} = 0.24 \times 10^{-9}$ m²/s (Demmink et al., 1997), the equilibrium constants of equilibria 20–25 given in Table 2 and the rate constants $k_{1,1}^m$ (m: m0, m1, and m2) determined below from absorption experiments with relatively low P_{H_2S}, given in Table 1. Given the observation that ferric chelate diffusivity depends on mass rather than charge (Wubs and Beenackers, 1993; Demmink et al., 1997), $D_B^{(m0)} = D_B^{(m1)} = D_B^{(m2)}$. For the diffusivity of the μ-oxo dimers, D_B^d, an estimation is used based on Wilke–Chang (see, for instance, Reid et al., 1987), assuming that the molar volume of the μ-oxo dimer is twice that of the monomeric species, $D_B^d = 0.15 \times 10^{-9}$ m²/s. Leaist and Hao (1994) observed that, for ferrous EDTA, an uncomplexed ligand has the same
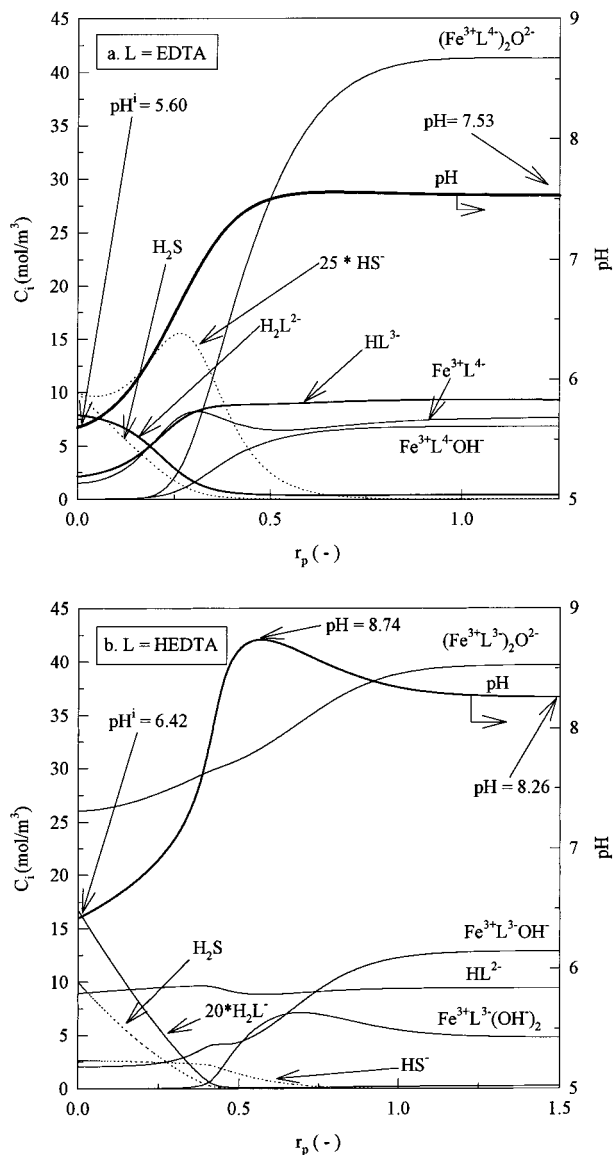
Figure 3. E_A as a function of pH, $C_{A,L}^i = 0.010$ kmol/m³, $\bar{C}_{Fe(III)} = 0.097$ kmol/m³, $T = 294$ K. Symbols: experimental data from Wubs and Beenackers (1994); closed, ferric EDTA; open, ferric HEDTA. Lines calculated with $D_A = 1.44 \times 10^{-9}$ m²/s (Haimour and Sandall, 1984), $D_B^m = 0.24 \times 10^{-9}$ m²/s, $D_B^d = 0.15 \times 10^{-9}$ m²/s, and equilibrium constants given by Gustafson and Martell (1963); see Table 2. E1, E1a (ferric EDTA), and H1 (ferric (HEDTA) calculated from the set of eqs 7 and 12. E1a: $D_B^d = D_B^m$, showing the relative small effect of D_B^d/D_B^m. Lines E2a, E2b, H2a, H2b, H2c, and EH2 calculated from eq 42. EH2: all ferric chelates assumed reactive ($C_B = C_{Fe(III)}$). Ferric EDTA: E2a and E2b both monohydroxylated and μ-oxo dimer reactive, nonhydroxylated ferric EDTA assumed unreactive ($C_B = C_B^{(m1)} + 2C_B^d$). E2a: $\nu_B = 1$. E2b: $\nu_B = 2$. Ferric HEDTA: H2a, dihydroxylated ferric HEDTA and μ-oxo dimer reactive ($C_B = C_B^{(m2)} + 2C_B^d$); H2b, dihydroxylated ferric HEDTA reactive only ($C_B = C_B^{(m2)}$); H2c, monohydroxylated and dihydroxylated ferric HEDTA reactive ($C_B = C_B^{(m1)} + C_B^{(m2)}$).

Figure 2b shows local concentration gradients for ferric HEDTA, $\overline{pH} = 8.26$. Here, the μ-oxo dimer does not completely dissociate at $r_p \to 0$. As a result of reactions 30 and 31, a local increase in pH occurs in the zone where $Fe^{3+}L_{HEDTA}^{3-}(OH^-)_2$ is consumed ($0.5 \leq r_p \leq 1.0$). Closer to the interface, the increase in pH is overcompensated by H^+ release, presumably due to reaction 41. Interestingly, as a result of the increasing pH, $C_B^{(m2)}$ shows a maximum value at $r_p = 0.6$.

Figure 3 shows experimental data from Wubs and Beenackers (1994), with lines E1 and H1 calculated from eqs 7 and 12, in combination with eq 6, for ferric EDTA and ferric HEDTA, respectively. All parameters used for these calculations were taken from elsewhere; see Table 1, Table 2, and Demmink et al. (1997). Although line E1 appears to underestimate the experimental observations, it reasonably matches over the entire range $4.5 \leq pH \leq 9.0$. Line E1a, calculated with $D_B^d = D_B^m$ (m: m0, m1, and m2) shows that the value of ratio D_B^d/D_B^m has relatively little impact on E_A. Line H1 appears to be shifted on the pH axis, but reasonably matches the experimental trends.

Given the high $C_{A,L}^i$, Wubs and Beenackers (1994) assumed the absorption data shown in Figure 3 to be a result of instantaneous reaction. This assumption may very well be valid for ferric EDTA. As shown in Figure 2a, close to the interface, practically all ferric EDTA is reduced, even though the μ-oxo dimer is assumed to react through dissociation ((22) and (23)) only. For ferric HEDTA, however, the assumption of instantaneous

Figure 2. Near interface concentration profiles, calculated from eqs 7 and 12. For readability, some species are not shown, although these were incorporated in the calculation. $C_{A,L}^i = 0.010$ kmol/m³, $\bar{C}_{Fe(III)} = 0.097$ kmol/m³, $\bar{C}_{ligand} = 1.1 \bar{C}_{Fe(III)}$, $T = 294$ K with $D_B^m = 0.24 \times 10^{-9}$ m²/s, $D_B^d = 0.15 \times 10^{-9}$ m²/s. Equilibrium constants ((20)−(25)) from Gustafson and Martell (1963); see Table 2; $k_{1,1}$ values from Table 1. (a) $L = $ EDTA. (b) $L = $ HEDTA.

diffusivity as iron chelate. For readability, some ionic components, for instance Na^+, Cl^-, and ferrous chelates, are not shown in Figure 2, although they were included in the calculation.

In Figure 2a, where $L = $ EDTA, local concentration gradients resulting from mass-transfer limitation during H_2S absorption are shown. It is seen that as H_2S penetrates into the liquid element, $C_B^{(m1)}$ decreases as a result of reactions 28 and 29. Although, following the suggestion by Philip and Brooks (1974) and Wubs and Beenackers (1994), the μ-oxo dimer is assumed to be unreactive toward H_2S, its interfacial concentration decreases due to local dissociation via reactions 22 and 23 and is completely converted. Also shown is a local decrease of pH from a bulk value $\overline{pH} = 7.53$ to an interfacial value $pH^i = 5.60$, even though the excess of ligand ($C_{EDTA} = 1.1 \times C_{Fe(III)}$) has some buffering effect; see equilibrium 25.
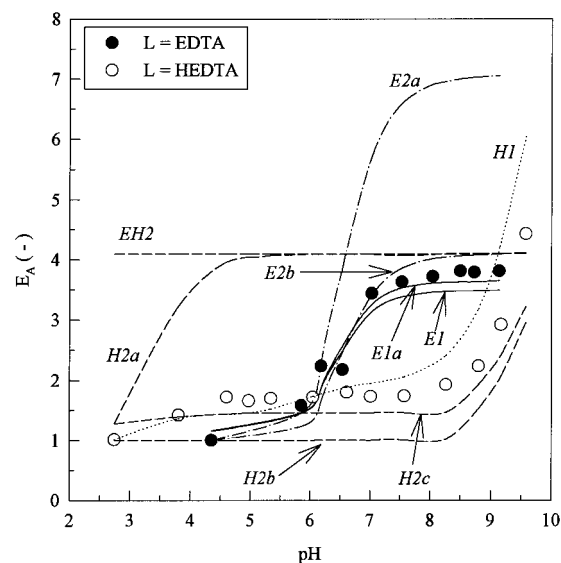
reaction is not correct; as shown in Figure 2b, only $Fe^{3+}L^{3-}_{HEDTA}(OH^-)_2$ is completely reduced.

Lines EH2, E2a, E2b, H2a, H2b, and H2c in Figure 3 were calculated from the approximate expression for instantaneous irreversible reaction given by DeCoursey and Thring (1989):

$$E_{A,\infty} = q_A \frac{\sqrt{r_B}}{2} + \sqrt{\frac{q_A^2 r_B}{4} + q_A + 1} \qquad (42)$$

with

$$q_A = \frac{C_B}{\nu_B C^i_{A,L}} \quad \text{and} \quad r_B = \frac{D_B}{D_A} \qquad (43)$$

which was shown to approximate exact, but implicit, solutions within 3% (DeCoursey and Thring, 1989). Here, C_B pertains to the concentration ferric chelate which is reactive to H_2S.

Assuming that all ferric chelate consuming steps (i.e., reactions 26, 29 and 30, and 27, 29, and 31) take place within the reaction zone, ν_B is set to $\nu_B = 2$ for all lines, except E2a, where $\nu_B = 1$. Hence, in the latter case, it is assumed that reactions 27, 29, and 31 take place in the bulk of the liquid. As shown in Figure 3, line E2a, this assumption is unlikely to be correct.

The hypothetical line EH2 in Figure 3, was calculated from eq 42 under the assumption of instantaneous reaction of all ferric complexes: $C_B = C_{Fe(III)}$. For ferric EDTA, E_A calculated from this approach matches the experimental data for pH $\geq$ 8, which appears to be consistent with Figure 2a, where both $Fe^{3+}L^{4-}_{EDTA}(OH^-)$ and $(Fe^{3+}L^{4-}_{EDTA})_2O^{2-}$ were completely consumed near the interface. A good approximation over the entire range $4.5 \leq$ pH ≤ 8.5 from eq 42 is obtained by setting $C_B = C^{(m1)}_B + 2C^d_B$, line E2b. The (apparent) reactivity of the μ-oxo dimer may result from local dissociation via reactions 22 and 23; also see Figure 2a.

For the reactive absorption of H_2S into ferric HEDTA solutions, line H2a in Figure 3 was calculated with eq 42, $C_B = C^{(m1)}_B + 2C^d_B$. This approach appears to overestimate E_A for pH < 9, indicating that, for ferric HEDTA, the assumption of instantaneous reaction of μ-oxo dimer does not hold. Line H2b, obtained from eq 42 setting $C_B = C^{(m2)}_B$ underestimates the observed values, whereas line H2c, with $C_B = C^{(m2)}_B + C^{(m1)}_B$, appears to give a reasonable approximation. These observations suggest that for ferric HEDTA the μ-oxo dimer is indeed not reactive to H_2S (as suggested earlier; see Philip and Brooks, 1974; Wubs and Beenackers, 1994). However, as shown in Figure 2b, neither the assumption that the ferric HEDTA μ-oxo dimer does not at all contribute to the H_2S absorption under the conditions of Figure 3 nor the assumption of instantaneous reaction of $Fe^{3+}L^{3-}_{HEDTA}(OH^-)$ is correct. One should therefore be careful in distinguishing the reactivity of these complexes. As shown by line H1, however, local dissociation 22 and 23 may sufficiently account for the observed H_2S absorption rates.

The results of the comprehensive model, lines E1 and H1, indicate that the absorption of H_2S, accompanied by instantaneous reaction, is primarily determined by (interfacial) ferric chelate chemistry. Other factors that

may influence the absorption rate, such as in situ formation of solid particles (Mehra and Sharma, 1988; Demmink et al., 1994) or polysulfides (Wubs and Beenackers, 1994; Clarke et al., 1994) appear to be less important under the conditions of Figure 3. The substantial and improbable difference in $D_{Fe(III)}$ values for ferric EDTA and HEDTA, as determined by Wubs and Beenackers (1994), now appears to result from using too simple ferric chelate chemistry, in combination with mass transfer. The complete reduction of the ferric EDTA μ-oxo dimer at pH = 7.53, and partial reduction of the ferric HEDTA μ-oxo dimer at pH = 8.26 (Figure 2), are difficult to predict a priori, and for this reason the use of a more comprehensive mass-transfer model, represented by eqs 6 and 7 with boundary conditions (14)–(19), should be preferred over the simplified model, represented by eq 42.

3.2. Low-Pressure Regime. Figure 4 shows near interface concentration profiles for $C^i_{A,L} = 1.0$ mol/m³. Despite this relatively low $C^i_{A,L}$, considerable interfacial concentration and pH gradients occur, although less than in Figure 2. Figure 4a shows for ferric EDTA, that, although the μ-oxo dimer is assumed to be unreactive to H_2S, its local concentration gradient is steeper than the gradient of the reactive component $Fe^{3+}L^{4-}_{EDTA}(OH^-)$. Apparently, equilibria 22 and 23 play an important role, and the rate constants k_{-22} and k_{-23} may affect the rate of H_2S conversion. Figure 5 shows the experimental results of Wubs and Beenackers (1994) for $C^i_{A,L} = 1.0$ mol/m³. Table 1 gives the $k_{1,1}$ values determined from Figure 5 (eqs 7, 12, and 6), where it should be realized that the values for $k^{(m1)}_{1,1}$ are maximum values, since it is still not possible to exclude some direct reactivity of μ-oxo dimers.

It appears that for ferric HEDTA the $k_{1,1}$ values determined here from eqs 7, 12, and 6 are in the same order of magnitude as those reported by Wubs and Beenackers (1994). Also, the equilibrium constants of ferric HEDTA, determined from gas absorption data by Wubs and Beenackers (1994), are very close to the actual values; see Table 2. Apparently, for ferric HEDTA, under the conditions of Figure 5, near interface dissociation of the μ-oxo dimer has little impact on the gas absorption rate. This is consistent with the relative small μ-oxo dimer concentration gradient shown in Figure 4b. However, given the results of both relative high $C^i_{A,L}$ (Figure 3) and relative low $C^i_{A,L}$, the use of approximate models (for instance, DeCoursey, 1974; DeCoursey and Thring, 1989; Westerterp et al., 1984) for the absorption of H_2S, accompanied by reaction 1, cannot be recommended for either ferric EDTA or HEDTA.

For ferric EDTA, a maximum in the observed E_A occurs at pH $\approx$ 7. This maximum does not follow from the equilibrium concentrations of ferric species shown in Figure 1 and was earlier (Wubs and Beenackers, 1994) ascribed to the in situ formation of sulfur particles, or the role of polysulfides. However, as seen in Figure 5, line E3, such a maximum may also follow from near interface concentration gradients shown in Figure 4a. As shown in Figure 1a, at pH < 6, most ferric EDTA is present in its hydrated form, $Fe^{3+}L^{4-}_{EDTA}$, which appears to have a relatively low reactivity to H_2S. At pH > 6, most ferric EDTA is present either as reactive hydroxylated species or as a μ-oxo dimer, whose reactivity now appears to be low. At pH $\approx$ 7, the μ-oxo dimer
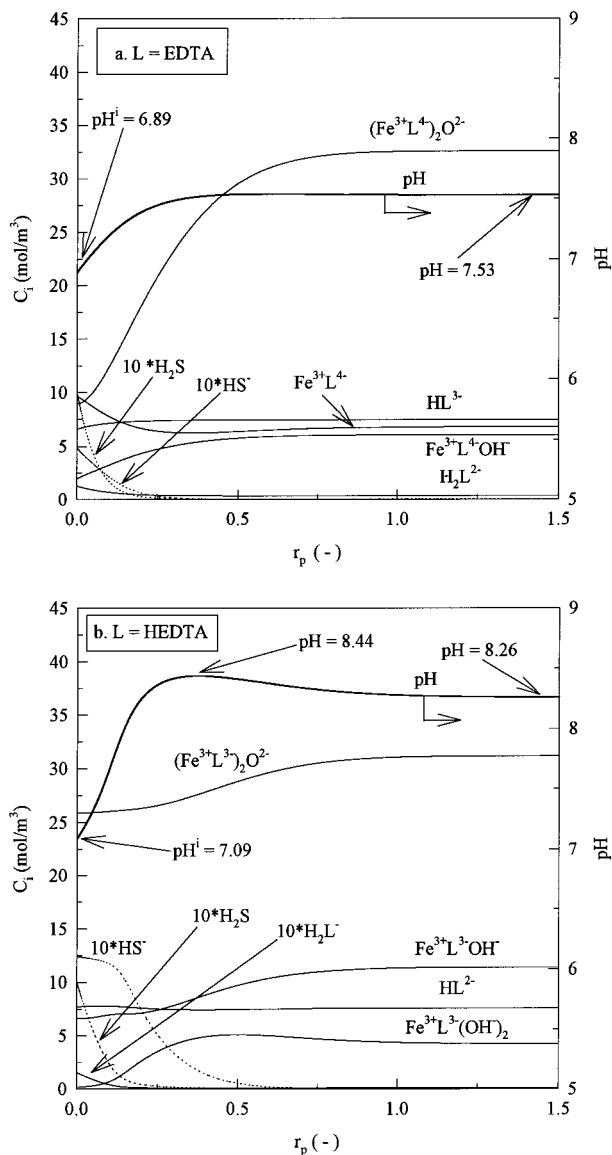
Figure 4. Near interface concentration profiles, calculated from eqs 7 and 12. For readability, some species are not shown, although these were incorporated in the calculation. $C_{A,L}^i = 1.0 \times 10^{-3}$ kmol/m³, $\bar{C}_{Fe(III)} = 0.078$ kmol/m³, $T = 294$ K, $C_{ligand} = 1.1\ C_{Fe(III)}$, $T = 294$ K. $D_A = 1.44 \times 10^{-9}$ m²/s (Haimour and Sandall, 1984), $D_B^m = 0.24 \times 10^{-9}$ m²/s, $D_B^m = 0.15 \times 10^{-9}$ m²/s (Demmink et al., 1997), $k_L = 1.27 \times 10^{-4}$ m/s. Equilibrium constants for equilibria 20–25 from Gustafson and Martell (1963); see Table 2; $k_{1,1}$ values in 1. (a) Ferric EDTA; (b) ferric HEDTA.

dissociates via equilibrium 23, while at pH > 7 equilibrium 22 becomes more important. The observed maximum E_A therefore supports the above assumption (also see Wubs and Beenackers, 1994) that the ferric EDTA μ-oxo dimer reacts via equilibria 22 and 23 only.

The importance of the μ-oxo dimer dissociation rate also follows from the hypothetical line E4 in Figure 5, calculated with $k_{1,1}$ of Table 1 and $k_{23} = 10$ m³/(mol s), half the value given in Table 2. It is seen that the value of k_{23} has significant impact on the reactive absorption rate of H_2S.

The sequence in reactivity

$$Fe^{3+}L_{HEDTA}^{3-}(OH^-)_2 \gg Fe^{3+}L_{EDTA}^{4-}(OH^-) \gg$$

$$Fe^{3+}L_{HEDTA}^{3-}(OH^-)$$
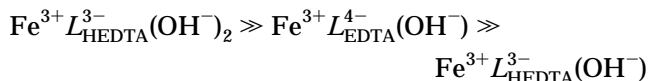
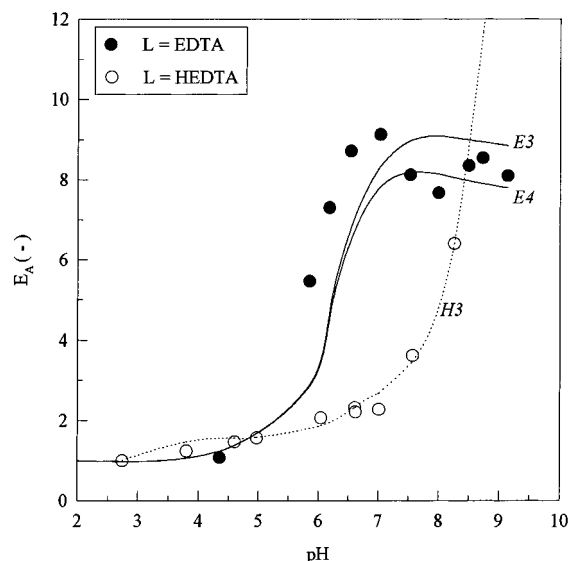reported by Wubs and Beenackers (1994) *qualitatively*

Figure 5. E_A as a function of pH, $C_{A,L}^i = 1.0 \times 10^{-3}$ kmol/m³, $\bar{C}_{Fe(III)} = 0.078$ kmol/m³, $T = 294$ K. Symbols: experimental data of Wubs and Beenackers (1994); closed, ferric EDTA; open, ferric HEDTA. Lines E3, E4, and H3: calculated from eqs 7 and 12, with $D_B^m = 0.24 \times 10^{-9}$ m²/s, $D_B^d = 0.15 \times 10^{-9}$ m²/s. Equilibria constants and formation rates of equilibria 20–22 and 25 given in Table 2. Line E3 and E4 ferric EDTA, $k_{1,1}^{(m1)} = 250$ m³/(mol s). E3: $k_{23} = 20$ m³/(mol s) (Wilkins and Yelin, 1969). E4: hypothetical line with $k_{23} = 10$ m³/(mol s). H3: ferric HEDTA, $k_{1,1}^{(m2)} = 1.5$ m³/(mol s), $k_{1,1}^{(m2)} = 600$ m³/(mol s).

still appears to hold, except that $k_{1,1}^{(m2)}$ (HEDTA) and $k_{1,1}^{(m1)}$ (EDTA) are now of the same order of magnitude:

$$Fe^{3+}L_{HEDTA}^{3-}(OH^-)_2 > Fe^{3+}L_{EDTA}^{4-}(OH^-) \gg$$
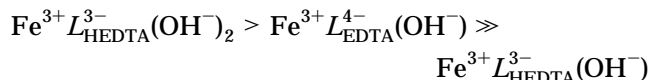
$$Fe^{3+}L_{HEDTA}^{3-}(OH^-)$$

This observation indicates that the number of hydroxy groups is less important than the pH at which a species is abundant. From Figure 1 it follows that the reactive species $Fe^{3+}L_{EDTA}^{4-}(OH^-)$ and $Fe^{3+}L_{HEDTA}^{3-}(OH^-)_2$ are formed at approximately the same pH (pH > 7). Also, it can be seen that the total number of negatively charged oxygen donors may play a role. Both $Fe^{3+}L_{HEDTA}^{3-}(OH^-)_2$, with three $-CH_2COO^-$ and two OH^-, and $Fe^{3+}L_{EDTA}^{4-}(OH^-)$, with four $-CH_2COO^-$ and one OH^-, have five negatively charged oxygen groups, whereas $Fe^{3+}L_{HEDTA}^{3-}(OH^-)$, with three $-CH_2COO^-$ and one OH^-, and $Fe^{3+}L_{EDTA}^{4-}$, with four $-CH_2COO^-$, have only four.

Conclusions

A comprehensive mass transfer with chemical reaction model, based on penetration theory, has been developed for the oxidative absorption of H_2S into aqueous solutions of ferric chelates and was tested with experimental data for ferric EDTA and HEDTA from Wubs and Beenackers (1994). It has been demonstrated that near interface concentration gradients influence the gas absorption rate to a high extent, which cannot be understood from general, approximate models from literature (Westerterp et al., 1984; DeCoursey, 1974; DeCoursey and Thring, 1989). It appears that the experimental data by Wubs and Beenackers (1994) are more consistent with literature equilibrium constants (Gustafson and Martell, 1963; Martell and Smith, 1982)

and literature diffusion coefficients (Wubs and Been-ackers, 1993; Demmink et al., 1997) than previously assumed.

As it has now been demonstrated from the experimental data of Wubs and Beenackers (1994) that the reactivity of the μ-oxo dimer is likely to be much lower than the reactivity of the hydroxylated species. Some direct reactivity can, however, not be excluded. Near interface interconversion of the μ-oxo dimer to reactive ferric chelate is important, since it provides an extra source of reactant. For ferric EDTA at relative high $C_{A,L}^i$ and pH > 7, this implies that practically all ferric species may be considered reactive, while for ferric HEDTA at relatively high $C_{A,L}^i$ this is not the case. Generally, for determining the rate of absorption of H_2S approximate expressions (for instance, DeCoursey, 1974; DeCoursey and Thring, 1989; Westerterp et al., 1984) should be treated with caution and the comprehensive approach presented here should be preferred.

Acknowledgment

Nomenclature

a = specific surface (m^2/m_L^3)
C = concentration ($kmol/m^3$)
D = diffusivity (m^2/s)
E_A = chemical enhancement factor; see eq 6
$E_{A,\infty}$ = chemical enhancement factor at instantaneous reaction; see eq 42
J_A = specific absorption rate of gas A ($mol/(m^2\ s)$)
$\bar{J}_A$ = average specific absorption rate of gas A, eq 4 ($mol/(m_L^2\ s)$)
k_L = liquid-side mass-transfer coefficient (m/s)
$k_{1,1}$ = reaction rate constant defined by eqs 33, 36, and 39 ($m^3/(mol\ s)$)
K_e (e = 1, 2 ...) = equilibrium constants, with e pertaining to equation number: ($kmol/m^3$) (eqs 20, 21, and 25); ($m^3/kmol$) (eq 22); ( ) (eq 23)
K_W = water ionization constant ($=C_{H^+}C_{OH^-}$) (mol^2/m^6)
L = ligand
n = number of carboxylic acid groups of ligand
r_B = diffusivity ratio defined in eq 43
r_p = relative penetration depth, see eq 10
R = gas constant ($=8.314$) ($J/(mol\ K)$)
R_A = reaction rate for component A ($mol/(m^3\ s)$)
q_A = stoichiometric ratio defined in eq 43
t = time (s)
T = temperature (K)
x = distance from gas–liquid interface (m)
y = length of polysulfide chain (S_y^{2-}, y = 2–7),
z = ion charge

Greek Symbols

Γ_i = dimensionless diffusivity coefficient of component i, eq 9
ν = stoichiometry
θ = average contact time in Higbie's penetration theory, eq 3 (s)
τ = dimensionless time, eq 11
ξ_i = dimensionless concentration of component i, eq 8

Super- and Subscripts

A = pertaining to gas-phase reactant, H_2S
B = pertaining to reactive ferric chelate
d = pertaining to μ-oxo dimer

e = pertaining to equilibrium or forward rate constant
$-e$ = pertaining to backward rate constant
Fe(II) = pertaining to ferrous chelate
Fe(III) = pertaining to total ferric chelate
G = gas phase
i = species i (subscript)
i = interface (superscript)
j = species j
L = liquid phase
m = species m (subscript)
m = pertaining to monomeric species (superscript)
m0 = pertaining to monomeric species $Fe^{3+}L^{n-}$
m1 = pertaining to monomeric species $Fe^{3+}L^{n-}OH^-$
m2 = pertaining to monomeric species $Fe^{3+}L^{n-}(OH^-)_2$

Ligands

DTPA = diethylenetriaminepentaacetic acid
EGTA = ethylene bis(oxyethylenenitrilo)tetraacetate
EDTA = ethylenediaminetetraacetic acid
HEDTA = hydroxyethylethylenediaminetriaacetic acid
NTA = nitrilotriacetic acid

Literature Cited

Asai, S.; Konishi, Y.; Yabu, T. Kinetics of absorption of hydrogen sulfide into aqueous ferric sulfate solutions. *AIChE J.* **1990**, *36*, 1331-1338.

Asai, S.; Nakamura, H.; Aikawa, H. Absorption of hydrogen sulfide into aqueous solutions of ferric chloride. *J. Chem. Eng. Jpn.* **1997**, *30*, 500−506.

Caldin, E. F.; Gold, V. *Proton Transfer Reactions*; Chapman and Hall: New York, 1975.

Cantrall, R. LO-CAT and LO-CAT II Applications and technology update. In *Sulfur Recovery Conference*, Austin, TX; Gas Research Institute: Chicago, IL, 1997; Vol. 8.

Clarke, E. T.; Solouki, T.; Russell, D. H.; Martell, A.; McManus, D. Transformation of polysulfidic sulfur to elemental sulfur in a chelated iron, hydrogen sulfide oxidation process. *Anal. Chim. Acta* **1994**, *299*, 97−111.

CRC Handbook of Chemistry and Physics, 60; CRC Press Inc.: Boca Raton, FL, 1980.

DeBerry, D. W. Rates and mechanism of reaction of hydrogen sulfide with iron chelates, gas research institute topical report. Technical Report 93/0019; Gas Research Institute: Chicago, IL, 1993.

DeBerry, D. W. Chemical evolution of liquid redox processes. *Environ. Prog.* **1997**, *16*, 193−199.

DeBerry, D. W.; Petrinec, B.; Trofe, T. New insights from investigation of fundamental mechanisms of liquid redox chemistry. In *Liquid Sulfur Recovery Conference*, Austin, TX; Gas Research Institute: Chicago, IL, 1991.

DeCoursey, W. J. Absorption with chemical reaction, development of a new relation of the Danckwerts model. *Chem. Eng. Sci.* **1974**, *29*, 1867−1872.

DeCoursey, W. J.; Thring, R. W. Effects of unequal diffusivities on enhancements factors for reversible and irreversible reaction. *Chem. Eng. Sci.* **1989**, *44*, 1715−1721.

Demmink, J. F.; Beenackers, A. A. C. M. Oxidation of ferrous nitrilotriacetic acid with oxygen: a model for oxygen mass transfer parallel to reaction kinetics. *Ind. Eng. Chem. Res.* **1997**, *36*, 1989−2005.

Demmink, J. F.; Wubs, H. J.; Beenackers, A. A. C. M. Oxidative absorption of hydrogen sulfide by a solution of ferric nitrilotriacetic acid complex in a co-current down flow column packed with SMV-4 static mixers. *Ind. Eng. Chem. Res.* **1994**, *33*, 2989−2995.

Demmink, J. F.; van Gils, I. C. F.; Beenackers, A. A. C. M. Absorption of nitric oxide into aqueous solutions of ferrous chelates accompanied by instantaneous reactions. *Ind. Eng. Chem. Res.* **1997**, *36*, 4914−4927.

Giles, T. W. R.; Smith, J. W.; Tombalaikan, A. S. Kinetic study of the catalytic oxidation of hydrogen sulphide in industrial waste streams. *Waste Process. Recycl.* **1994**, 229−239.

Gustafson, R. L.; Martell, A. E. Hydrolytic tendencies of ferric chelates. *J. Phys. Chem.* **1963**, *67*, 576−582.

Haimour, N.; Sandall, O. C. Molecular diffusivity of hydrogen sulfide in water. *J. Chem. Eng. Data* **1984**, *29*, 20−22.

Koch, S.; Ackermann, G.; Schüller, K. Über ternäre komplexe mit aminopolycarbonsäuren und sulfid. *Z. Chem.* **1986**, *26*, 339.

Leaist, D. G.; Hao, L. Traces diffusion of some metal ions and metal EDTA complexes in aqueous sodium chloride solutions. *J. Chem. Soc., Faraday Trans* **1994**, *90*, 133−136.

Lonergan, M. C.; Lieberman, M.; Lewis, N. S. Mechanistic studies of and redox sensors for the liquid redox process. In *1995 GRI Sulfur Recovery Conference*, Austin, TX; Gas Research Institute: Chicago, IL, 1995.

Martell, A. E.; Smith, R. M. *Critical Stability Constants*; Plenum Press: New York, 1982.

Mehra, A.; Sharma, M. M. Absorption of hydrogen sulfide in aqueous solutions of iodides containing iodine: enhancement in rates due to precipitated sulfur. *Chem. Eng. Sci.* **1988**, *43*, 1017−1081.

Nagl, G. J. Controlling H_2S emissions. *Chem. Eng.* **1997**, 125−131.

Neumann, D. W.; Lynn, S. Oxidative absorption of H_2S and O_2 by iron chelate solutions. *AIChE J.* **1984**, *30*, 62−69.

Newman, J. S. *Electrochemical Systems*; Prentice Hall Inc.: Englewood Cliffs, NJ, 1973.

Neyaglov, A. A.; Digurov; N. G. Bukharkina, T. V.; Mazgarov, A. M.; Fakhriev, A. M. Kinetics and reaction mechanism of the liquid phase oxidation of hydrogen sulphide by a chelate complex of trivalent iron. *Kinet. Katal.* **1991**, *32*, 485−489.

Oostwouder, S. P.; Hodge, V. B. Sulferox process technology and application update. In *GRI Sulfur Recovery Conference*, Austin, TX; Gas Research Institute: Chicago, IL, 1995.

Philip, C. V.; Brooks, D. W. Iron(III)chelate complexes of hydrogen sulphide and mercaptans in aqueous solutions. *Inorg. Chem.* **1974**, *13*, 384−386.

Reid, R. C.; Prausnitz, J. M.; Poling, B. E. *The properties of gases and liquids*, *4*; McGraw-Hill: New York, 1987.

dos Santos Afonso, M.; Stumm, W. Reductive dissolution of iron-(III)(hydr)oxides by hydrogen sulfide. *Langmuir* **1992**, *8*, 1671−1675.

Schugar, H. J.; Hubbard, A. T.; Anson, F. C.; Gray, H. B. Electrochemical and spectral studies of dimeric iron(III) species. *J. Am. Chem. Soc.* **1969**, *91*, 71−77.

Tsonopoulos, C.; Coulson, D. M.; Inman, L. B. Ionization constants of water pollutants. *J. Chem. Eng. Data* **1976**, *21*, 190−193.

Westerterp, K. R.; van Swaaij, W. P. M.; Beenackers, A. A. C. M. *Chemical reactor design and operation*; Wiley and Sons: New York, 1984.

Wilkins, R. G.; Yelin, R. E. The kinetics of monomer-dimer interconversion of iron(III) ethylene diaminetetraacetate and related chelates. *Inorg. Chem.* **1969**, *8*, 1470−1473.

Wubs, H. J. *Application of Iron Chelates in Hydrodesulphunsation*, Ph.d. Thesis, University of Groningen, Groningen, The Netherlands, 1994.

Wubs, H. J.; Beenackers, A. A. C. M. Kinetics of the oxidation of ferrous chelates of EDTA and HEDTA in aqueous solutions. *Ind. Eng. Chem. Res.* **1993**, *32*, 2580−2594.

Wubs, H. J.; Beenackers, A. A. C. M. Kinetics of absorption of hydrogen sulfide into solutions of ferric EDTA and HEDTA. *AIChE J.* **1994**, *40*, 433−444.

Yao, W.; Millero, F. J. Oxidation of hydrogen sulfide by hydrous Fe(III) oxides in seawater. *Marine Chem.* **1996**, *52*, 1−16.